THE ASTROPHYSICAL JOURNAL, 454:394–403, 1995 November 20

FOUR NEWLY IDENTIFIED SOURCES WITH 21 MICRON EMISSION

SUN KWOK
Department of Physics and Astronomy, University of Calgary, Calgary, Alberta, Canada T2N 1N4; kwok@iras.ucalgary.ca
BRUCE J. HRIVNAK
Department of Physics and Astronomy, Valparaiso University, Valparaiso, IN 46383; bhrivnak@exodus.valpo.edu
AND
T. R. GEBALLE
Joint Astronomy Center, Hilo, HI 96720; tom@jach.hawaii.edu
Received 1995 February 1; accepted 1995 May 11

ABSTRACT

Mid-infrared spectroscopy and near- and mid-infrared photometry have been obtained for four carbon-rich cool *IRAS* sources whose *IRAS* low-resolution spectra are similar to those of proto-planetary nebulae (PPNs) possessing the unusual 21 μm emission feature. The 21 μm feature is detected in all four sources, nearly doubling the number of known 21 μm emitters. The energy distributions of these objects show the characteristic "double-peaked" structure, confirming that they are PPNs. Broad features near 7.7 and 11.3 μm similar to the unidentified infrared features (UIRs) seen in carbon-rich planetary nebulae (PNs) are also detected, suggesting a chemical link between these PPNs and PNs. The presence of the 21 μm feature appears to be correlated with the presence of unusually strong 3.4–3.5 μm features. Possible scenarios for the evolution of these emission features in the PPN phase are discussed.

Subject headings: circumstellar matter — infrared: stars — planetary nebulae: general — stars: carbon

1. INTRODUCTION

Over the last decade, it has been recognized that mass loss on the asymptotic giant branch (AGB) has major effects on the formation of planetary nebulae (PNs). Many observable characteristics (e.g., halos, molecular envelopes) of PNs can be traced back to the circumstellar envelopes of their AGB progenitors (Kwok 1982). The large infrared excesses observed in PNs certainly originate in the expanded remnants of the AGB envelopes (Kwok 1990; Zhang & Kwok 1991). The detections in PNs of the 9.7 μm silicate and the 11.3 μm SiC features, both commonly observed in AGB stars, provide additional evidence of the link between AGB stars and PNs (Aitken & Roche 1982; Zhang & Kwok 1990).

On the other hand, the infrared spectra of PNs also show features not found in AGB stars (see, e.g., Lenzuni, Natta, & Panagia 1989). The most prominent are the family of unidentified infrared (UIR) features at 3.3, 6.2, 7.7, 8.6, and 11.3 μm, which are commonly attributed to the polycyclic aromatic hydrocarbon (PAH) molecules (Allamandola, Tielens, & Barker 1985). It is well documented that the 3.3 μm feature observed in the *L*-band window is closely correlated with the presence of the 11.3 μm feature observed by the *IRAS* Low Resolution Spectrometer (LRS) (Jourdain de Muizon, d'Hendecourt, & Geballe 1989), and the 6.2 and 7.7 μm features (Cohen et al. 1989) probably also are closely correlated with the above. The UIR features are particularly strong in PNs with large infrared excesses, especially those with WC 11 central stars (Kwok, Hrivnak, & Langill 1993).

The molecules responsible for the UIR features must either be synthesized during the transition from the AGB to the PN phase or be produced in the AGB atmosphere but not excited there. In either case, it is useful to study the infrared spectra of young PNs and transition objects between AGB stars and PNs (or proto–planetary nebulae [PPNs] in order to understand the origin of the UIR features. Recently, detections of a strong, broad emission feature at 21 μm and unusually strong 3.4–3.5 μm and 6–9 and 12 μm emission features in several cool *IRAS* sources which are PPNs have been reported (Kwok, Volk, & Hrivnak 1989; Hrivnak & Kwok 1991a; Geballe & van der Veen 1990; Geballe et al. 1992; Buss et al. 1990). The 21 μm feature was found initially in the *IRAS* LRS database, and has since been confirmed by both airborne (Omont 1993) and ground-based (Barlow 1993) observations. Optical spectroscopy has indicated that all the 21 μm emission sources are carbon rich (Hrivnak 1995), suggesting that the carrier of the feature is a carbon-based molecule. Many of the detections of the unusual shorter wavelength features have been made in the course of following up the 21 μm feature and the "normal" UIR features (Buss et al. 1990; Geballe et al. 1992).

Only five 21 μm emitters have been identified thus far. To understand the relationship of this feature to the other infrared emission features and to post-AGB evolution, it is important to identify additional 21 μm sources among cool *IRAS* sources. In this paper we report ground-based discoveries of the 21 μm feature in four new sources, along with additional spectroscopic and photometric data.

2. *IRAS* LOW-RESOLUTION SPECTRA

The *IRAS* LRS spectra of a number of cool *IRAS* sources were examined at the University of Calgary *IRAS* Data Analysis Facility. Details of the processing procedure are given in Volk et al. (1991). Figure 1 shows the LRS spectra of IRAS 05113+1347, IRAS 20000+3239, and IRAS 22223+4327, together with the previously known 21 μm source IRAS 07134+1005. The LRS spectra were observed in two sections, a blue section from 8 to 15 μm with resolution $\lambda/\Delta\lambda \sim 40$ and a red section from 13 to 23 μm with resolution ~ 20. A linear baseline has been removed in each band of the spectra. The spectra have been recalibrated using the spectra of seven bright stars as the flux standards (Volk & Cohen 1989). These spectra

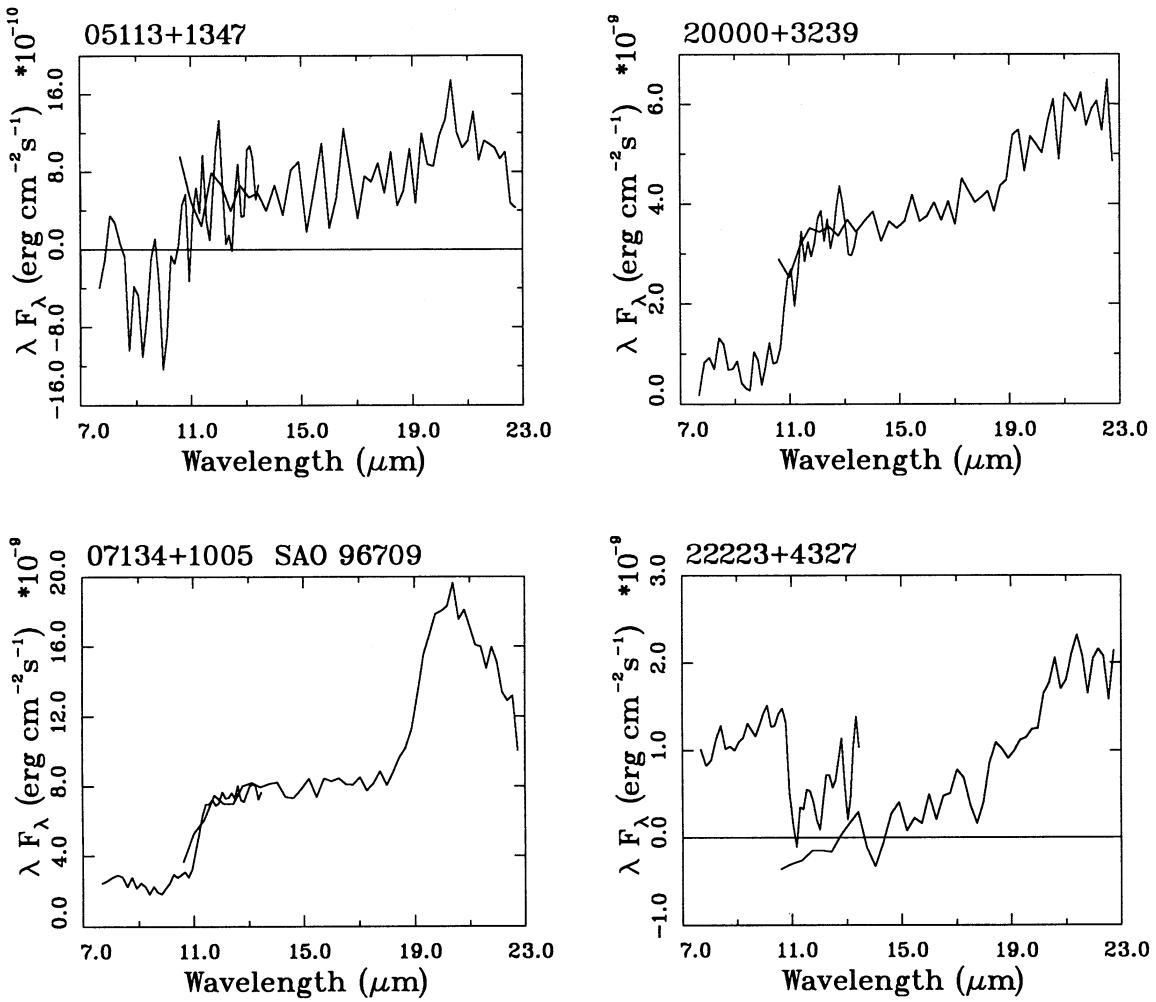

FIG. 1.—*IRAS* LRS spectra of three new 21 μm sources: IRAS 05113+1347, IRAS 20000+3239, and IRAS 22223+4327. The spectrum of IRAS 22223+4327 has been smoothed over three channels. The LRS spectrum of the strong, previously identified 21 μm source IRAS 07134+1005 is also shown for comparison.

have not been flux-calibrated using the *IRAS* Point Source Catalog (PSC) fluxes. In the case of IRAS 22223+4327, the spectrum was also smoothed over three channels using the "boxcar" method.

Although the signal-to-noise ratios of all the spectra are low for three new sources, IRAS 05113+1347 and IRAS 20000+3239 show the characteristic plateau between 12 and 18 μm, and each shows hints of a rise at ~20 μm, suggesting the presence of the 21 μm feature (see IRAS 07134+1005 for comparison).

3. OBSERVATIONS

3.1. *Mid-Infrared Spectroscopy*

Mid-infrared spectra of the above three *IRAS* 21 μm candidates and a fourth candidate, IRAS 05341+0852 (known to have unusually strong 3.4–3.5 μm emission), and four other cool *IRAS* sources, also thought to be transition objects but lacking evidence for the 21 μm feature, were obtained at the 3.8 m United Kingdom Infrared Telescope (UKIRT), using the facility instrument CGS3. CGS3 is a 32 channel cooled grating spectrometer, which can be used in the 7–24 μm range. The spectral resolving powers were ~50 at 10 μm and ~72 at 20 μm.

Two of the 21 μm candidates (IRAS 20000+3239 and IRAS 22223+4327) were observed in 1991 May 25, and the two others (IRAS 05113+1347 and IRAS 05341+0852) were observed on 1991 September 9 and again on 1993 November 3. The other four objects (IRAS 17150−3224, IRAS 19477+2401, IRAS 20136+1309, and IRAS 20406+2943) were measured in 1991 May and June. All of these observations were made using a 30″ EW chop and nod, and apertures of diameter either 5.″5 (1991) or 3.″9 (1993). All spectra were sampled every one-third resolution element. Various stars, including BS 7525 (γ Aql), BS 2491 (α CMa), and BS 1457 (α Tau) were used for flux calibration. In order to better correct for the strong terrestrial water absorption lines in the 20 μm band, the spectra of the four 21 μm candidates and their standards were cross-correlated to measure the spectral shift between them. The spectrum of the standard was then shifted by the determined amount and divided into the source spectrum in order to better cancel the terrestrial absorption features.

3.2. *Mid-Infrared Photometry*

Mid-infrared photometry of three of the four 21 μm candidates was obtained at the 3.6 m Canada-France-Hawaii Tele-

TABLE 1

MID-INFRARED PHOTOMETRY

A. CFHT (1986 May 25)

	Wave Band (μm)								
IRAS Name	7.8	8.7	9.8	10.3	*N*	11.6	12.5	*Q*	25
20000+3239.....	2.70	2.35	1.95	1.66	1.75	0.60	0.45	−1.49	−2.5

B. UKIRT (1989 November 1)

	Wave Band						
IRAS Name	8.75	9.6	10.3	*N*	11.6	12.5	19.5
05113+1347.....	4.05	3.67	2.94	2.78	1.93	1.84	0.34
22223+4327.....	4.38	4.35	3.96	3.60	2.87	2.24	−0.19

scope (CFHT) and UKIRT. The observing dates and filters are given in Table 1. A single-channel Ge:Ga bolometer was used for these observations, and a 6″.0 aperture and east-west throw of 20″ at a frequency of 12.5 Hz were used in the UKIRT observations. Infrared standard stars were observed throughout each night to transform the program star observations to the standard system.

The *IRAS* sources were located by manually scanning an area equal to 4 times the *IRAS* error box, centered on the *IRAS* position. The broad *N* filter was used for detection. In all cases, the sources were within the *IRAS* error boxes. We believe that the association of these sources with the *IRAS* sources is unambiguous, based upon the similarity of positions and the expected low degree of source confusion at 10 μm, and the similarity in flux and color to the *IRAS* sources.

The standardized magnitudes for the program objects are listed in Table 1, where the bandpasses or central wavelengths of the filters are listed as column headings. Based upon the signal-to-noise ratios of our observations and the uncertainties in standardization and extinction, we estimate the uncertainties in these data to be ±0.10 mag at the shorter wavelengths, and ±0.15 mag, ±0.15 mag, and ±0.20 mag at 12.5, 20, and 25 μm, respectively. The measured *N* and *Q* magnitudes were found to be consistent with the *IRAS* [12] and [25] magnitudes.

3.3. *Near-Infrared Photometry*

Near-infrared observations were obtained at UKIRT and, in the case of IRAS 20000+3239, were kindly obtained by R. Joyce with the 1.3 m telescope at Kitt Peak National Observatory (KPNO). At UKIRT, *JHKL'M* photometry was obtained using the UK9 InSb photometer. Apertures of 8″ and 12″ were used. The KPNO observations were made with the BT InSb photometer, using a 15″ aperture and a throw of 40″ in declination. The *M* filters at KPNO and UKIRT are narrowband filters. For the InSb observations, the systematic errors are estimated to be less than 10%. The derived magnitudes are given in Table 2.

3.4. *Visible Photometry*

Visible photometry of IRAS 20000+3239 and IRAS 22223+4327 was obtained with the University of Hawaii (UH) 0.6 m telescope located on Mauna Kea. The telescope was equipped with a single-channel photometer with GaAs detector. The *UBV* and *RI* observations were transformed to the standard Johnson and Cousins photometric systems, respectively, through the observations of nightly standard stars. IRAS 05113+1347 and IRAS 20000+3239 were kindly observed by H. C. Harris, using a CCD on the US Naval Observatory (USNO) 1.0 m telescope in Flagstaff, Arizona. These *BV* and *I* observations were also transformed to the Johnson and Cousins systems, respectively, with an uncertainty of a couple of percent due to the use of somewhat nonstandard filters. In Table 3 are listed the standard magnitudes of these three sources. The two sets of observations of IRAS 20000+3239 show a difference of 0.2 mag, which may be due to variability of the source.

4. RESULTS

4.1. *Mid-Infrared Spectroscopy*

The CGS3 mid-infrared spectra of the new 21 μm candidates are displayed in Figure 2. The 21 μm feature is evident in the spectra of all four, the flux level between 19 and 22 μm lies significantly above a straight-line fit to the flux interpolated from the spectrum just shortward of 19 μm and to just longward of 22 μm. Estimates of the total fluxes contained in the 21 μm feature are given in Table 4. Except for IRAS 05341+0852, the feature is superposed on a steeply rising continuum. Substructure in the feature may be present, in particular near 20.0 μm (see the spectra of IRAS 05341+0852 and IRAS 20000+3239), but requires additional measurements for con-

TABLE 2

NEAR-INFRARED PHOTOMETRY

IRAS Name	*J*	*H*	*K*	*L*	*L'*	*M*	Observatory	Observing Date
05113+1347.....	8.98	8.34	8.06	...	7.56	7.21	UKIRT	1989 Feb 15
20000+3239.....	7.93	7.03	6.73	5.83	...	5.20	KPNO	1987 Oct 07
22223+4327.....	7.89	7.46	7.25	...	6.99	6.75	UKIRT	1989 Aug 17

TABLE 3

VISIBLE PHOTOMETRY

IRAS Name	*U*	*B*	*V*	R_C	I_C	Observatory	Observing Date
05113+1347.....	...	14.54	12.41	...	10.26	USNO	1989 Oct 01
20000+3239.....	17.53	16.13	13.39	11.80	10.32	UH	1989 Aug 24
	...	15.94	13.17	...	10.16	USNO	1988 Oct 18
22223+4327.....	11.41	10.61	9.69	9.15	8.63	UH	1989 Aug 24

firmation. Substructure in the 20 μm region of IRAS 22272+5432 and IRAS 04296+3429 has been suggested by Barlow (1993).

The 8–13.5 μm spectra of these sources generally resemble those of the previously known 21 μm sources, with broad features peaking near 8 and 12 μm. There appears to be little correlation between the strengths of these peaks and that of the 21 μm feature. The well-known 11.3 μm UIR feature (probably arising from out-of-plane CH bending; Allamandola et al. 1985) is very prominent in IRAS 05341+0852, can also be seen in IRAS 20000+3239, and may contribute to the spectra of the other two sources but is not obvious in them. Likewise, the 7.7 μm C—C stretching mode probably contributes to the 8 μm emission features in these objects (Allamandola et al. 1985). In IRAS 05341+1347, the 12 μm feature shows definite structure, with an emission peak at 12.5 μm in addition to the feature at 11.4 μm.

In Figure 3 are plotted the UKIRT CGS3 spectra of the other four cool *IRAS* sources. In none of them is the 21 μm feature evident. The quality of the these 20 μm spectra is lower than those of Figure 2 and, with the exception of IRAS 20136+1309, the existence of the 21 μm feature at the level at which it was detected in the spectra of Figure 2 cannot be ruled out. However, the broad 9.7 μm silicate feature is clearly evident in emission in IRAS 20136+1309, and is seen in absorption in the other three. The published LRS spectrum of IRAS 17150−3224 and extracted LRS spectrum of IRAS 20406+2943 confirm the silicate absorption feature in these two objects. We note that the silicate emission feature in IRAS 20136+1309 is very similar to the silicate feature in the

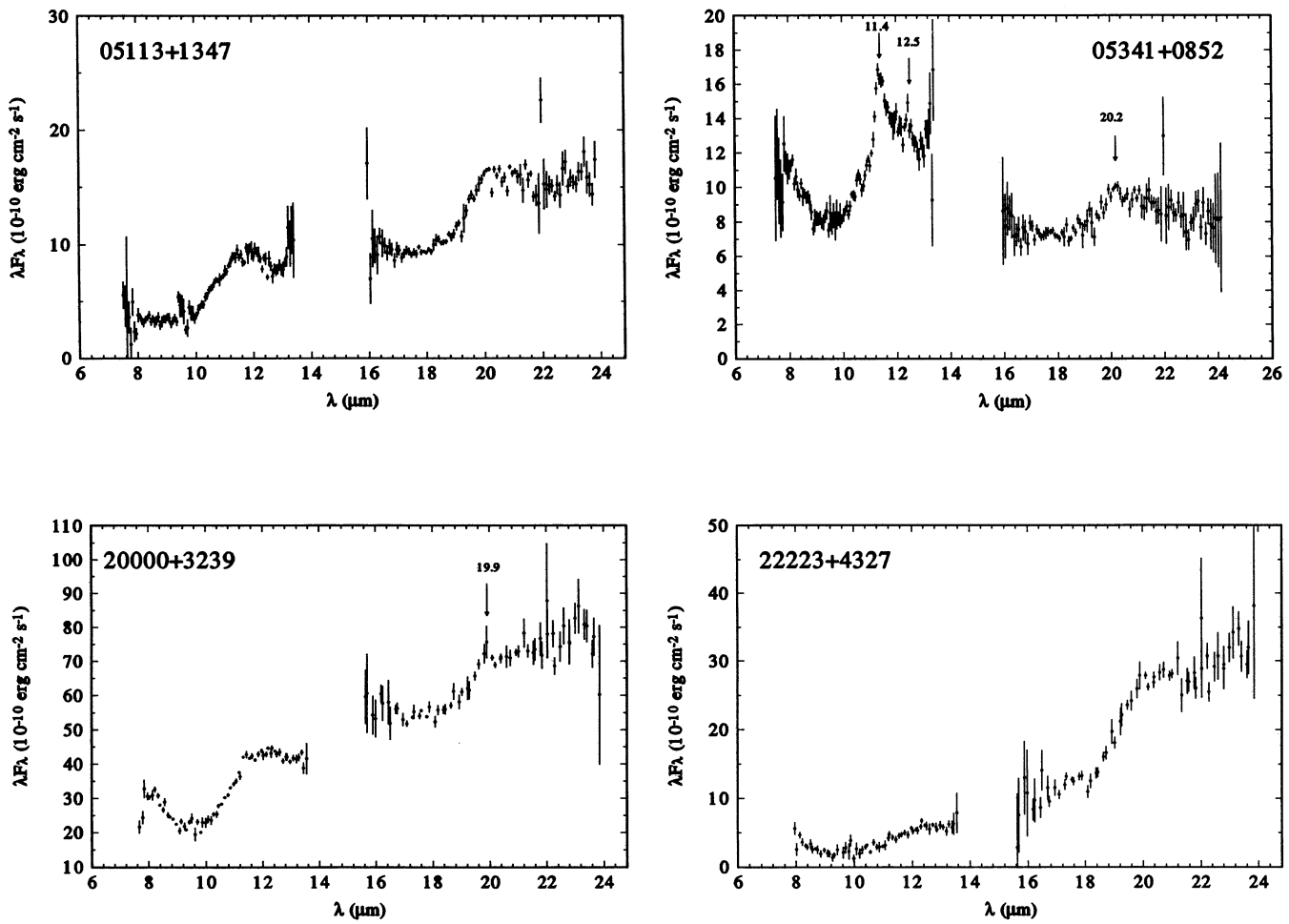

FIG. 2.—UKIRT CGS3 spectra of the four 21 μm candidates

TABLE 4

FLUX IN THE 21 MICRON FEATURE

	IRAS SOURCE			
	05113+1347	05341+0852	20000+3239	22223+4327
Flux (ergs cm^{-2} s^{-1}).....	3.1×10^{-11}	1.3×10^{-11}	7.9×10^{-11}	7.4×10^{-11}

oxygen-rich PPN IRAS 18095+2704 (Hrivnak, Kwok, & Volk 1988). It is likely that these four are oxygen-rich objects. Molecular-line OH emission has been observed in IRAS 17150−3224 (te Lintel Hekkert 1991), IRAS 20406+1943, and perhaps IRAS 19477+2401 (Likkel 1989), which supports the ideal that they are oxygen-rich objects.

IRAS 20000+3239 has also been observed in the mid-infrared from the Kuiper Airborne Observatory (KAO) by Omont et al. (1995). The KAO spectrum of this object is plotted in Figure 4 for comparison with the CGS3 data. The first band of the KAO spectrum has lower spectral resolution than the CGS3 data, but shows the same general shape, with an emission feature superposed on a rising continuum. The KAO flux integrated across the 21 μm *IRAS* filter profile is approximately 20% lower than the *IRAS* photometry (Szeczerba et al. 1995), roughly the same amount by which it falls below the UKIRT CGS3 spectrum. The accuracy of the KAO absolute calibration is ~10% for sources much smaller than the 30″ beam (Omont et al. 1995). It is unclear whether this 20% difference between the KAO and the CGS3 data implies variation in the source or arises from a calibration problem. The KAO spectrum is seen to rise to a peak at 28–30 μm; the presence of a 30 μm emission feature in several of these sources is described later.

4.2. *Spectral Energy Distribution*

The observed spectral energy distributions (SEDs) of the four new 21 μm sources are plotted in Figure 5, along with best-fit SEDs from a spherical radiative transfer model. The effective temperatures used (see Table 5) for the central stars

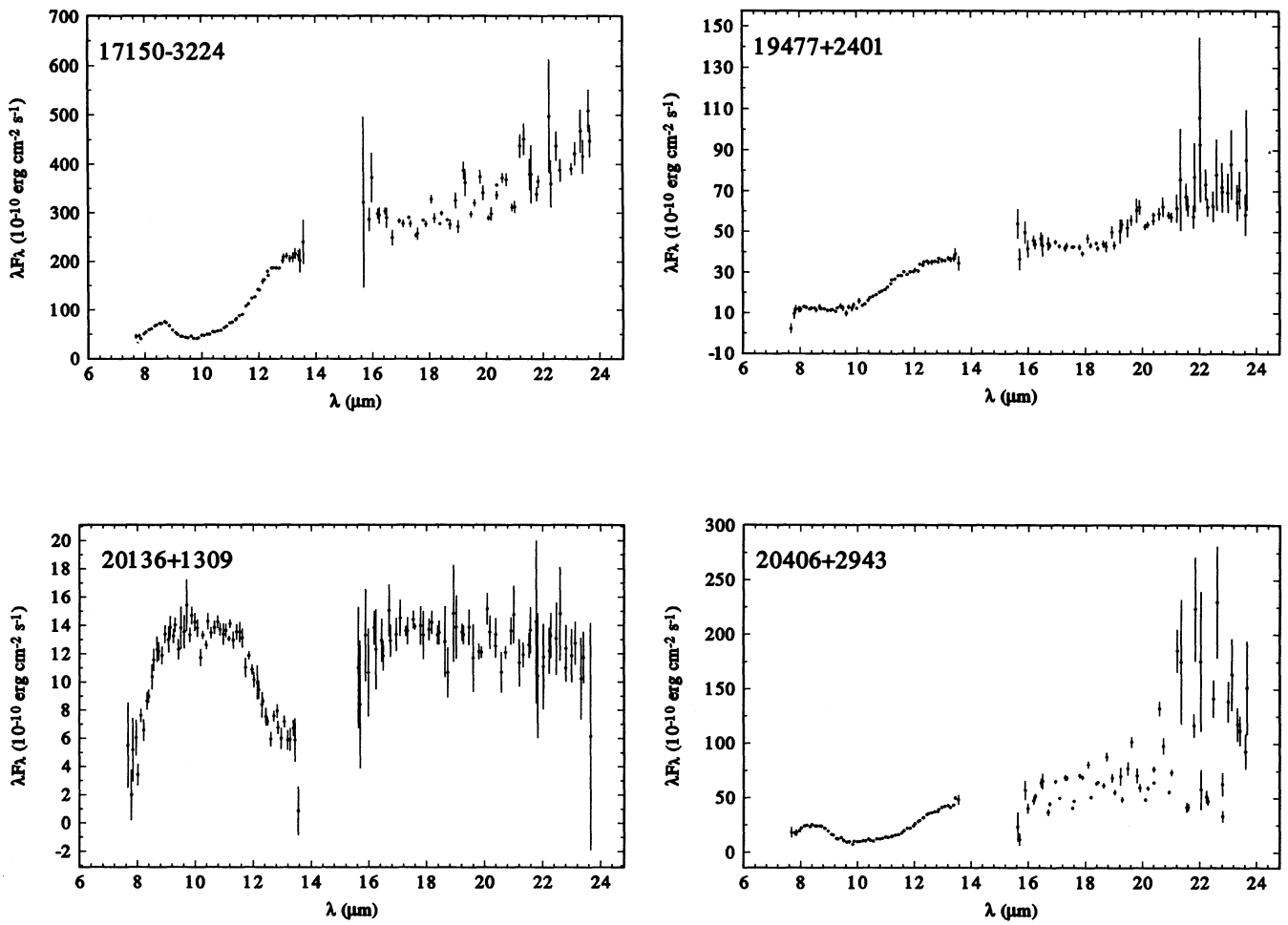

FIG. 3.—UKIRT CGS3 spectra of four other cool *IRAS* sources

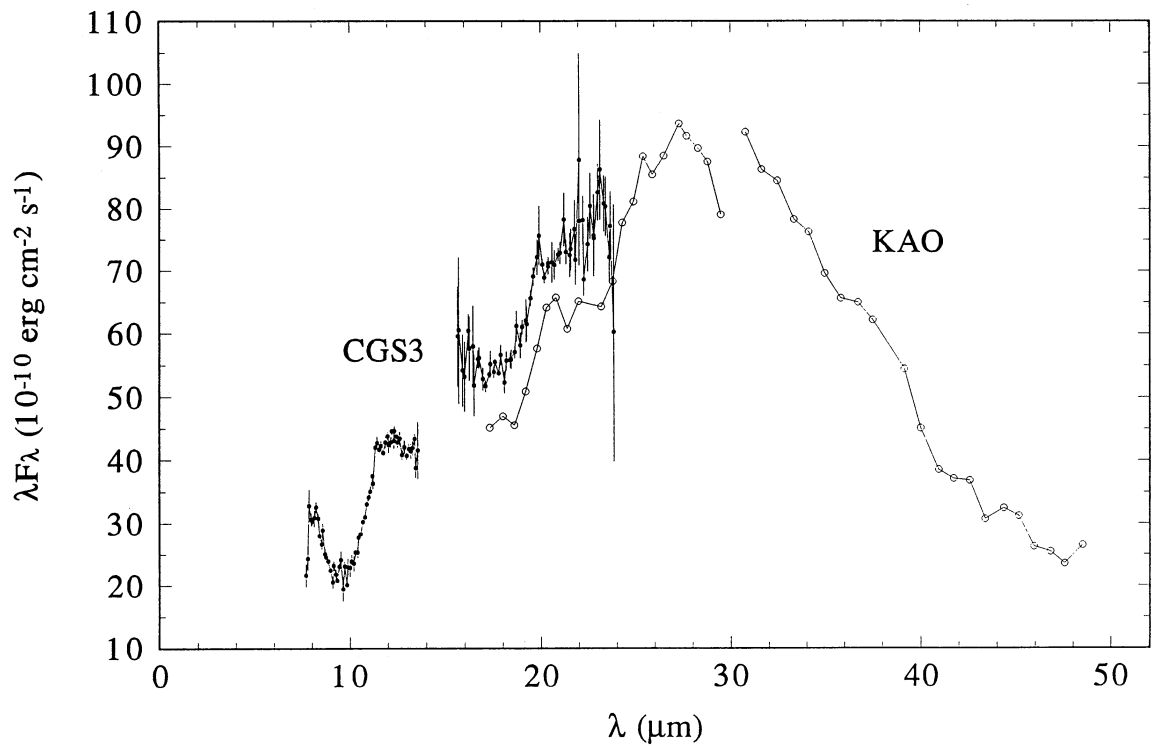

FIG. 4.—KAO spectrum (*open circles*) of IRAS 20000+3239 plotted together with the UKIRT CGS3 data (*filled circles*). The two sets of data would agree better if the flux of the first (short-wavelength) KAO band were multiplied by a factor of 1.2 (see text).

are consistent with the spectral classifications of these stars by Hrivnak (1995). The opacity function in the model includes contributions from amorphous carbon grains of size greater than 50 Å. PAHs of sizes between 5 and 10 Å, and an empirical opacity function designed to fit the 21 and 30 μm features (see Szczerba et al. 1995 for details). The template for the 21 μm feature is the bright 21 μm source IRAS 07134+1005, and the bumps at 21 μm in the model SEDs in Figure 5 are the result of this template opacity function.

All four sources show a clear separation between photospheric and circumstellar components, typical of PPNs. The colors of the objects are redder than expected for their G spectral types, with contributions from both circumstellar and interstellar reddening. In order to include the effects of interstellar reddening, we have corrected the photometry data for extinction expected in the directions to the objects (Neckel & Klare 1980). The models in Figure 5 are made to fit the corrected photometry observations.

TABLE 5

MODEL AND DERIVED PARAMETERS

IRAS Source	L_*/D^2 ($L_\odot$ kpc^{-2})	T_* (K)	Total Flux (ergs cm^{-2} s^{-1})	z/D (pc kpc^{-1})
04296+3429[a]	555	5000	1.8×10^{-08}	−158
05113+1347	130	5300	4.2×10^{-09}	−247
05341+0852	105	7000	3.4×10^{-09}	−211
07134+1005[a]	1719	6600	5.5×10^{-08}	174
20000+3239	547	5300	1.8×10^{-08}	21
22223+4327	361	6000	1.2×10^{-08}	−201
22272+5435	2983	5300	9.5×10^{-08}	−44
23304+6147[a]	628	5000	2.0×10^{-08}	10

[a] Model parameters from Kwok et al. 1989.

5. DISCUSSION

5.1. *Common Properties of the 21 Micron Sources*

In Table 6, we have listed the complete sample of previously known and newly confirmed 21 μm sources. These nine objects form a unique class sharing the following properties:

1. All have F or G spectral types with luminosity class I (Hrivnak 1995).
2. All have "double-peaked" energy distributions, indicating the presence of a cool dust shell detached from the photosphere.
3. All are carbon-rich objects based on their optical spectra.
4. All six of those which have been observed show HCN emission (Omont et al. 1993).
5. Of the five sources for which near-infrared spectroscopy has been obtained, all show the 3.3 μm emission feature and three show unusually strong 3.4–3.5 μm emission.
6. A significant fraction of the 21 μm sources also show an emission feature at 30 μm.
7. With the exception of IRAS 20000+3239, all are located in the outer Galaxy.

The first two properties suggest that these objects belong to the class of recently discovered PPNs (Kwok 1993a). The spectral types and luminosity classes are consistent with their being transition objects between the AGB and PN phases. The detached dust shells represent remnants of the circumstellar envelopes ejected during the AGN, which are now dispersing into the interstellar medium. The carbon molecules observed in the optical spectra (Hrivnak 1995) suggest that the carrier of the 21 μm feature is carbon-based. The observed HCN emission is consistent with these being carbon-rich objects (Omont et al. 1993).

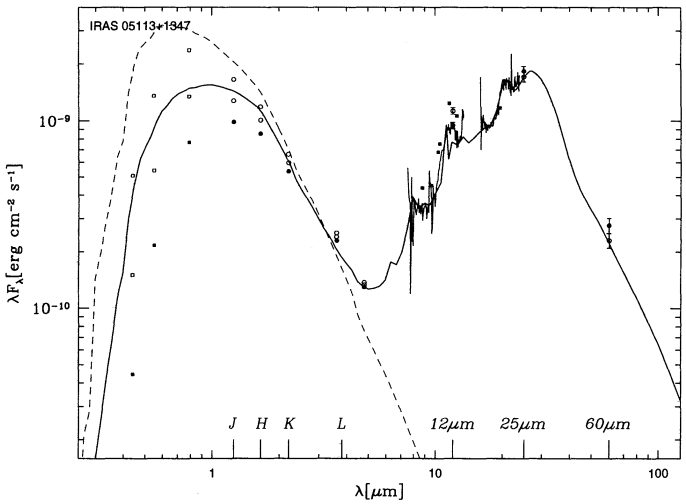

FIG. 5a

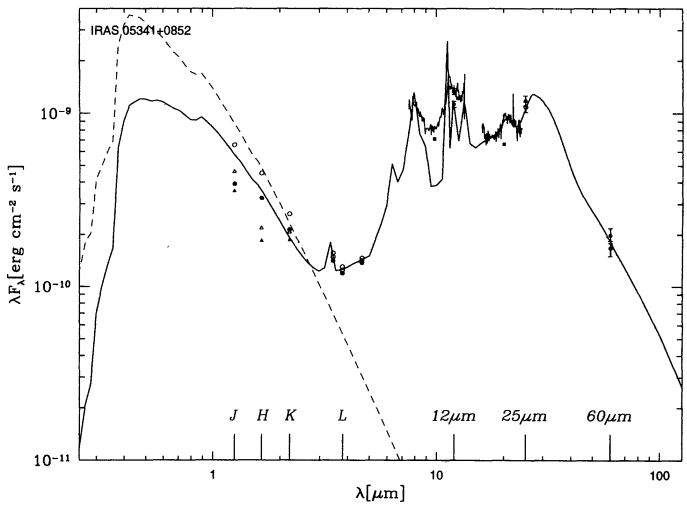

FIG. 5b

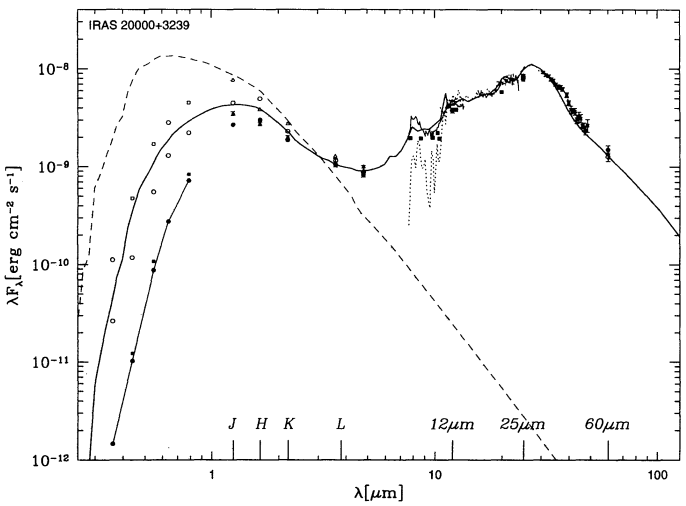

FIG. 5c

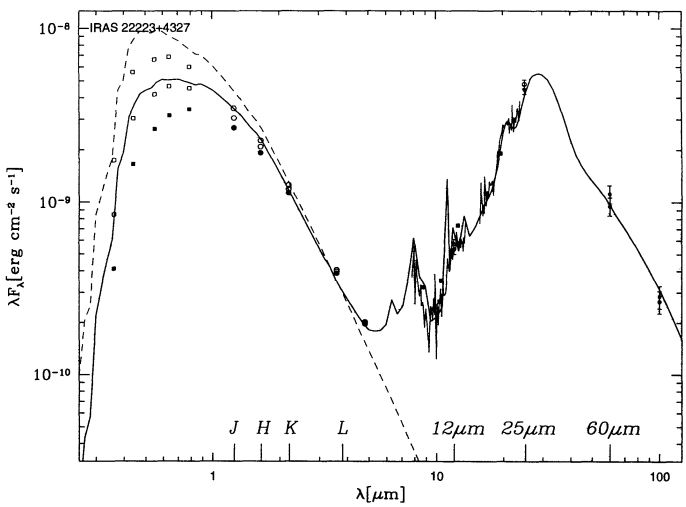

Fig. 5d

FIG. 5.—(*a*) Spectral energy distribution (SED) of IRAS 05113+1347. The solid symbols between 0.5 and 5 μm are ground-based photometric observations from this paper. The *IRAS* LRS is shown as dotted lines, and the CGS3 data as thin solid lines. Both sets of data have been adjusted slightly to agree with the color-corrected *IRAS* 12 and 25 μm fluxes. The dashed line is the assumed SED of the central star, and the solid line is the fit of the model curve to the observed SED. The effects on the observed photometry of correcting for $A_V = 1$ or 2 mag of interstellar extinction are shown as open symbols. Details of the fitting processes are described in Szczerba et al. (1995). (*b*) SED of IRAS 05341+0852. Symbols and curves are as described in (*a*). The near- and mid-IR photometry data are from Geballe & van der Veen (1990). The effects on the observed photometry of correcting for $A_V = 1$ or 2 mag of interstellar extinction are shown as open symbols. (*c*) SED of IRAS 20000+3239. The solid symbols between 0.5 and 5 μm are ground-based photometry observations from this paper and from Manchado et al. (1989). The effects on the observed photometry of correcting $A_V = 2$ or 3 mag of interstellar extinction are shown as open symbols. The crosses (some with error bars) are from KAO data. (*d*) SED of IRAS 22223+4327. The effects on the observed photometry of correcting for $A_V = 0.5$ or 1 mag of interstellar extinction are shown as open symbols.

5.2. *Luminosities and Core Masses of the* 21 *Micron Sources*

These sources are likely to be no more than a few kiloparsecs away, since eight out of the nine sources are located in the outer Galaxy and four of the nine have Galactic latitudes greater than 10°, yet are not expected to be at large distances above the plane. The latter point is quantified in Table 5, where we have listed z/D, where z is the distance above the plane and D is the distance. For reasonable values of z, the total luminosities for most of the sources are no more than a few times $10^3\ L_\odot$ (see Table 5), corresponding to core masses of $0.6\ M_\odot$ or less.

5.3. 21 *Micron Features and Unusual* 3.4–3.5 *Micron Emission*

The detection of strong 3.4–3.5 features in several of the 21 μm sources is particularly interesting. While the 3.3, 7.7, and 11.3 μm UIR features are commonly seen in PNs, the only PNs that show somewhat comparable 3.4–3.5 μm features are BD +30°3639, NGC 7027 (Geballe et al. 1985; Nagata et al. 1988), and IRAS 21282+5050 (de Muizon et al. 1986), all of which have large infrared excesses and are regarded as being very young. However, the profiles of the 3.4–3.5 μm features and the wavelengths of peak intensity are not exactly the same in these 21 μm sources as in the PNs. Furthermore, the ratios of the

TABLE 6

IRAS SOURCES WITH 21 MICRON EMISSION FEATURE

IRAS NAME	SPECTRAL TYPE[a]	GALACTIC COORDINATES		MOLECULAR FEATURE IN OPTICAL SPECTRA[a]	PAH-RELATED FEATURES (μm)
		l	*b*		
04296+3429.....	G0 Ia	166°2	−9°1	C_2, C_3	3.3, 3.4–3.5,[b] 7.7, 11.3
05113+1347.....	G8 Ia	188.9	−14.3	C_2, C_3	3.3,[c] 11.3
05341+0852.....	F[d]	196.2	−12.2	...	3.3, 3.4–3.5,[d] 7.7, 11.3
07134+1005.....	F5 I	206.7	10.0	C_2	3.3,[e] 6.9[f]
20000+3239.....	G8 Ia	69.7	1.2	C_2	7.7, 11.3
22223+4327.....	G0 Ia	96.7	−11.6	C_2, C_3	...
22272+5435.....	G5 Ia	103.3	−2.5	C_2, C_3[g]	3.3, 3.4–3.5,[b] 6.9,[f] 7.7, 11.3[h]
22574+6609.....	...	112.0	6.0	...	7.7, 11.3
23304+6147.....	G2 Ia	113.9	0.6	C_2, C_3	7.7, 11.3

[a] Hrivnak 1995.
[b] Geballe et al. 1992.
[c] Hrivnak, Kwok, & Geballe 1994.
[d] Geballe & van der Veen 1990.
[e] Kwok, Hrivnak, & Geballe 1990.
[f] Buss et al. 1990.
[g] Hrivnak & Kwok 1991b.
[h] Barlow 1993.

strengths of the 3.4–3.5 μm to the 3.3 μm features are much larger in these 21 μm sources.

It has been suggested that the normal 3.4–3.5 μm emission peaks seen in PNs are due to the hot bands of the fundamental 3.3 μm CH stretch (Barker, Allamandola, & Tielens 1987). However, the unusually strong 3.4–3.5 emission seen in the 21 μm feature–emitting PPNs cannot be attributed to hot bands (Geballe et al. 1992). Indeed, even the normal features probably do not have hot bands as their dominant contributor (Geballe et al. 1994). Moreover, the lack of ultraviolet flux from the central stars of PPNs with the 21 μm feature makes excitation of the emitting molecules to high vibrational levels unlikely. It now seems most likely that the emissions longward of the 3.3 μm feature are due to vibrations of aliphatic sidegroups (e.g., $-CH_2$, $-CH_3$) attached to PAHs (Jourdain de Muizon et al. 1989). An alternative theory is given by Webster (1991, 1992, 1993, 1995), who suggests that the 3.4–3.5 μm features (as well as the 21 μm feature) are due to vibrational transitions of the fulleranes ($C_{60}H_m$, $m = 1, 2, \ldots, 60$) and their ions.

In any event, it is tempting to associate the 3.4–3.5 μm features with the unidentified 21 μm emission feature. The three objects (IRAS 04296+3429, IRAS 05341+0852, IRAS 22272+5432) that show the strongest 3.4–3.5 μm emission features also possess the 21 μm feature. However, the strongest 21 μm source—IRAS 07134+1005—does not show the 3.4–3.5 μm features (Kwok, Hrivnak, & Geballe 1990), so this correlation cannot be considered to be perfect. We do note, however, that IRAS 07134+1005 differs from others in that it has the hottest central star (F5, while the others are all of G spectral type, except for IRAS 05341+0852, which lacks a precise spectral classification), and also the smallest HCN/CO intensity ratio (Omont et al. 1993). Also, IRAS 05113+1347 has only a weak 3.3 μm feature and no obvious 3.4–3.5 feature (Hrivnak, Kwok, & Geballe 1994).

5.4. *Evolutionary Scenarios*

Buss et al. (1990) suggest that the 21 μm feature could arise from hydrogenated amorphous carbon (HAC) grains, which are later shattered into PAH molecules by a fast wind at the beginning of the PN phase. HAC consists of a network of aromatic rings of various sizes bonded peripherally to polymeric or hydrocarbon species, and can be the precursor of PAH molecules (Duley & Williams 1986). Extreme carbon stars on the AGB are often featureless in the mid-infrared (Volk, Kwok, & Langill 1992), and their circumstellar envelopes could be made of HAC grains. Perhaps these grains are excited by visible photons during the transition from the AGB to the PN phase, creating the 21 μm feature, the "unusual" 3.4–3.5 μm emission, and the broad 6–9 and 12 μm plateaus. Then, as the HAC grains are reduced to smaller PAH molecules in the PN phase, the normal PAH features become dominant. In this scenario, the lack of PAH features and the strength of the 21 μm feature in IRAS 07134+1005 would suggest that this object is at an earlier stage of evolution than the other sources, and the molecule bearing the 21 μm feature (e.g., HAC) is yet to be transformed into PAH molecules. However, counter to this idea is the fact that IRAS 07134+1005 has the earliest spectral type and is therefore furthest along in its blueward evolution across the H-R diagram.

On the other hand, because the HAC grains are excited by visual (and UV) photons, and radiatively destroyed by UV, one might well account for the increase in strength of the 21 μm feature by the increase in visible and UV luminosity as the central star evolves to earlier spectral type, until destruction of the 21 μm–emitting material is nearly complete. A similar scenario might explain the evolution of the 6–9 and 12 μm features and the unusual 3.4–3.5 μm features. Based on the spectrum of IRAS 07134+1005, the carrier(s) of the 3.4–3.5 μm emission would have to be shorter-lived than the carrier(s) of the other features, because the 3.4–3.5 μm emission disappears prior to the disappearance of the 21 μm and the 6–9 and 12 μm emissions.

5.5. *Other Issues*

The detection of a 30 μm emission feature in four 21 μm sources (IRAS 07134+1005, IRAS 20000+3239, IRAS 22272+5435, and IRAS 23304+6147; Omont et al. 1995) suggests that these two features share some common origin. However, the 30 μm feature has been seen in AGB stars (e.g., IRC +10216) and PNs (e.g., IC 418) as well as in PPNs (Cox

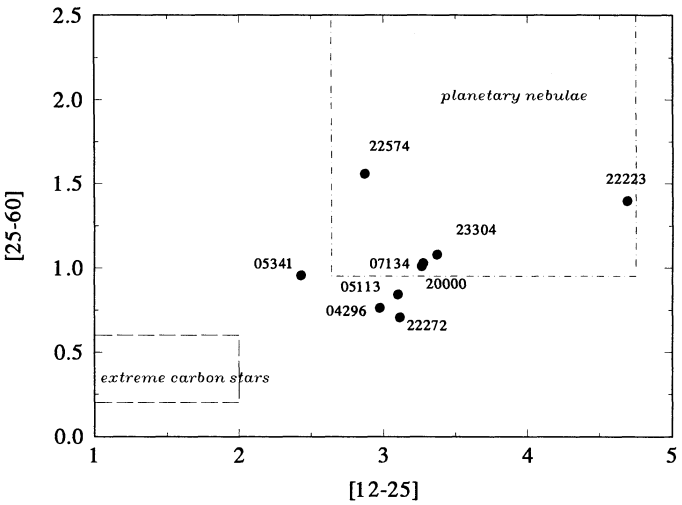

FIG. 6.—*IRAS* 12/25/60 μm color-color distribution of the nine 21 μm sources. Also plotted are the color regions occupied by planetary nebulae (Volk et al. 1991) and extreme carbon stars (Volk et al. 1992). The *IRAS* color indices are as defined by Walker & Cohen (1988).

1993), while the 21 μm feature thus far appears to be restricted to PPNs.

The fact that nearly all of the 21 μm sources are located in the outer Galaxy is unlikely to be a coincidence. It has been suggested that the carbon star to M star ratio increases from the inner to the outer Galaxy (Claussen et al. 1987; Kleinmann 1989). This could be the result of a metallicity gradient (especially O and N) in the Galaxy (Faúndez-Abans & Maciel 1986), leading to a higher formation rate for carbon stars with increasing radial distance from the Galactic center. One could imagine that the threshold for the formation of the 21 μm feature–bearing molecule/grain requires yet a higher C/O ratio, which is significantly enhanced in a lower metallicity environment.

It may be interesting to compare the infrared spectra of the 21 μm objects to those of RV Tauri stars, which are also post-AGB stars with cool dust envelopes (Bidelman 1989). However, the *IRAS* LRS spectra of RV Tauri stars either show silicate emission features, as seen in AC Her and U Mon, or unusual spectra, such as seen in RV Tauri and AR Pup (Kwok 1993b). While RV Tauri stars and the 21 μm sources may be in similar stages of stellar evolution, they clearly evolved from different progenitor stars.

It has been noted that the 21 μm sources are found in a restricted part of the *IRAS* color-color diagram (Omont et al. 1993; Hrivnak 1995). Figure 6 shows the distribution of the nine 21 μm sources listed in Table 6. Also plotted in Figure 6 are *IRAS* color regions occupied by the extreme carbon stars (Volk et al. 1992) and PNs (Walker et al. 1989; Volk et al. 1991). All the 21 μm sources have very red colors, redder than the most evolved carbon stars on the AGB. Six of the nine objects form a narrow locus of points on this diagram, suggesting a range of typical colors of 21 μm sources. The fact that their *IRAS* colors are intermediate between the reddest of carbon stars and PN is consistent with the suggestion that the 21 μm sources are objects in transition between the AGB and the PN phases (Kwok 1993a).

6. CONCLUSIONS

We have carried out ground-based spectroscopy and photometry of three *IRAS* sources that show possible 21 μm emission features in their LRS spectra, and spectroscopy of one additional candidate which displays strong 3.4–3.5 μm emission. A weak 21 μm feature was detected in all four objects. As a group, nine 21 μm sources now known share many common properties. They are all carbon-rich F or G supergiants, with at least five showing UIR features in the near-infrared. They all have detached dust envelopes, suggesting that they have suffered large-scale mass loss in the recent past (presumably on the AGB). The molecule responsible for the 21 μm feature is likely to be related to the molecular clusters/grains emitting the 3.4–3.5 μm features, for both sets of features are rare and they are usually seen together. These molecules are likely to have been synthesized in the AGB phase, with the broad plateaus and the 21 μm feature excited by the visible photons present during the transition to the PN phase. The identification of the chemical origin of this feature represents an interesting challenge in astronomical infrared spectroscopy.

We thank R. R. Joyce, H. C. Harris, and P. P. Langill for obtaining some of the photometric data reported in this paper. We are grateful to the staff of UKIRT for the support of their service observing program. UKIRT is operated by the Royal Observatories on behalf of the UK Particle Physics and Astronomy Research Council. This work is supported in part by a NASA Astrophysics Data Program grant (NAG 5-1223) and in part by a research grant from the Natural Sciences and Engineering Research Council.

REFERENCES

Aitken, D. K., & Roche, P. F. 1982, MNRAS, 200, 217
Allamandola, L. J., Tielens, A. G. G. M., & Barker, J. R. 1985, ApJ, 290, L25
Barker, J. R., Allamandola, L. J., & Tielens, A. G. G. M. 1987, ApJ, 315, L61
Barlow, M. J. 1993, in ASP Conf. Ser. 41, Astronomical Infrared Spectroscopy, ed. S. Kwok (San Francisco: ASP), 97
Bidelman, W. P. 1989, in Evolution of Peculiar Red Giant Stars, ed. H. R. Johnson & B. Zuckerman (Cambridge: Cambridge Univ. Press), 294
Buss, R. H., Jr., Cohen, M., Tielens, A. G. G. M., Werner, M. W., Bregman, J. D., Witteborn, F. C., Rank, D., & Sandford, S. A. 1990, ApJ, 365, L23
Claussen, M. J., Kleinmann, S. G., Joyce, R. R., & Jura, M. 1987, ApJS, 65, 385
Cohen, M., Tielens, A. G. G. M., Bregman, J., Witteborn, F. C., Rank, D. M., Allamandola, L. J., Wooden, D., & de Muizon, M. 1989, ApJ, 341, 246
Cox, P. 1993, in ASP Conf. Ser. 41, Astronomical Infrared Spectroscopy, ed. S. Kwok (San Francisco: ASP), 163
de Muizon, M., Geballe, T. R., Baas, F., & d'Hendecourt, L. B. 1986, ApJ, 306, L105
Duley, W., & Williams, D. A. 1986, MNRAS, 219, 859
Faúndez-Abans, M., & Maciel, W. J. 1986, A&A, 158, 228
Geballe, T. R., Joblin, C., d'Hendecourt, L. B., Jourdain de Muizon, M., Tielens, A. G. G. M., & Leger, A. 1994, ApJ, 434, L15
Geballe, T. R., Lacy, J. H., Persson, S. E., McGregor, P. J., & Soifer, B. T. 1985, ApJ, 292, 500
Geballe, T. R., Tielens, A. G. G. M., Kwok, S., & Hrivnak, B. J. 1992, ApJ, 387, L89
Geballe, T. R., & van der Veen, W. E. C. J. 1990, A&A, 235, L9
Hrivnak, B. J. 1995, ApJ, 438, 341
Hrivnak, B. J., & Kwok, S. 1991a, ApJ, 368, 564
———. 1991b, ApJ, 371, 631
Hrivnak, B. J., Kwok, S., & Geballe, T. R. 1994, ApJ, 420, 783
Hrivnak, B. J., Kwok, S., & Volk, K. 1988, ApJ, 331, 832
Jourdain de Muizon, M., d'Hendecourt, L. B., & Geballe, T. R. 1989, in Infrared Spectroscopy in Astronomy (ESA SP-290: Paris: ESA), 177
Kleinmann, S. G. 1989, in IAU Colloq. 106, Evolution of Peculiar Red Giant Stars, ed. H. R. Johnson & B. Zuckerman (Cambridge: Cambridge Univ. Press), 13
Kwok, S. 1982, ApJ, 258, 280
———. 1990, MNRAS, 244, 179
———. 1993a, ARA&A, 31, 63
———. 1993b, in ASP Conf. Ser. 45, Luminous High-Latitude Stars, ed. D. D. Sasselov (San Francisco: ASP), 348

Kwok, S., Hrivnak, B. J., & Geballe, T. R. 1990, ApJ, 360, L23
Kwok, S., Hrivnak, B. J., & Langill, P. P. 1993, ApJ, 408, 586
Kwok, S., Volk, K., & Hrivnak, B. J. 1989, ApJ, 345, L51
Lenzuni, P., Natta, A., & Panagia, N. 1989, ApJ, 345, 306
Likkel, L. 1989, ApJ, 344, 350
Manchado, A., Pottasch, S. E., Garcia-Lario, P., Esteban, C., & Mampaso, A. 1989, A&A, 214, 139
Nagata, T., Tokunaga, A., Sellgren, K., Smith, R. G., Onaka, T., Nakada, Y., & Sakata, A. 1988, ApJ, 326, 158
Neckel, Th., & Klare, G. 1980, A&AS, 42, 251
Omont, A. 1993, in ASP Conf. Ser. 41, Astronomical Infrared Spectroscopy, ed. S. Kwok (San Francisco: ASP), 87
Omont, A., Loup, C., Forveille, T., te Lintel Hekkert, P., Habing, H., & Sivagnanam, P. 1993, A&A, 267, 515
Omont, A., et al. 1995, ApJ, submitted
Szczerba, R., et al. 1995, in preparation
te Lintel Hekkert, P., Caswell, J. L., Habing, H. J., Haynes, R. F., & Norris, R. P. 1991, A&AS, 90, 327
Volk, K., & Cohen, M. 1989, AJ, 98, 1918
Volk, K., Kwok, S., & Langill, P. P. 1992, ApJ, 391, 285
Volk, K., Kwok, S., Stencel, R., & Brugel, E. 1991, ApJS, 77, 607
Walker, H. J., & Cohen, M., Volk, K., Wainscoat, R. J., &Schwartz, D. E. 1989, AJ, 98, 2163
Webster, A. 1991, Nature, 352, 412
———. 1992, MNRAS, 257, 463
———. 1993, MNRAS, 264, 121
———. 1995, MNRAS, in press
Zhang, C. Y., & Kwok, S. 1990, A&A, 237, 479
———. 1991, A&A, 250, 179